Optical breakdown in alkali halides*

A. Schmid† and P. Kelly
Physics Division, National Research Council, Ottawa, Canada, K1A 0S1

P. Bräunlich
Department of Physics, Washington State University, Pullman, Washington 99164
(Received 20 June 1977)

A theory of optical breakdown in dielectrics is presented and applied to NaCl and NaBr for wavelengths $0.172 \leq \lambda \leq 1.0642$ μm. It is based on multiphoton carrier generation and energy transfer from the radiation field to the lattice via polaron-photon absorption. This mechanism represents a clear alternative to avalanche breakdown models as no lattice impact ionization is involved. Breakdown field strengths calculated for various laser pulse lengths and frequencies, are fully corrected for the nonlinear refractive index n_2 as well as for contributions to the refractive index resulting from a sharp increase in polaron density during a damaging pulse. The results are in good agreement with experimental data obtained with nanosecond laser pulses.

I. INTRODUCTION

The electron avalanche model, since its introduction by Zverev *et al.*,[1] has apparently been remarkably successful in describing several experimentally observed optical-breakdown phenomena in dielectric solids. Although many details of the original concept have been modified extensively in recent years, the basic features remained: in the presence of an intense radiation field, electrons that are either initially available[2] in the conduction band or generated by single- or multiphoton carrier generation[3] are accelerated by simultaneously interacting with the photon field and the surrounding lattice vibrations. They may gain sufficient energy in successive photon-electron-phonon collisions to create additional free electrons by impact ionization of either impurities or lattice constituents (e.g., transitions of valence electrons into the conduction band). The ensuing increase in the free-electron concentration will in turn increase the total production rate of those electrons whose kinetic energy reaches the ionization limit ("hot" electrons). This process repeats itself until the resulting electron avalanche has reached such proportions that dielectric breakdown is inevitable.

The detailed processes that are expected to lead to hot electrons in a dielectric exposed to an intense flux of optical photons are presently still subject to much debate. Most theoretical approaches advanced in the literature have serious problems in explaining the magnitude of the avalanche ionization rate as a function of the optical field strength and, as a consequence, the breakdown field strength E_B.[2,4]

"Inverse bremsstrahlung" is commonly thought to be a mechanism by which, in the presence of an electric field E and of electron-phonon collisions, electrons are capable of gaining energy at a rate

$$\frac{d\epsilon}{dt} = \frac{e^2 \tau_c E^2}{m(1+\omega^2\tau_c^2)}, \tag{1}$$

where e is the charge of the electron, m its effective mass, τ_c the electron-phonon collision time, and ω the laser frequency.[5,6]

Inelastic electron-phonon collisions prevent rapid acceleration of the electrons and, as a result, almost all the energy absorbed from the radiation field is deposited into the lattice of the dielectric. According to Sparks,[4] the simple avalanche model suffers from its inability to simultaneously determine the magnitude of the ionization rate and its frequency dependence. To circumvent this considerable problem, Yablonovitch and Bloembergen[7] derived the ionization rate $W_i(E)$ for NaCl from experimental dc breakdown data. Their procedure was justified by measurements of the breakdown field strength E_B of various alkali halides at the CO_2 frequency which exhibited remarkable similarities with the dc data.[8] Surprisingly, the measured values of E_B in the same materials exhibited a dependence on the laser pulse length that could straightforwardly be explained by the very same $W_i(E)$ even at the Nd and ruby frequencies.[9,10] One simply had to assume dielectric breakdown occurred as soon as the electron avalanche had grown to a carrier density of about 10^{18} cm^{-3}. Similar behavior was observed in a number of other wide-band-gap materials (mostly alkali halides). As a consequence, the semiempirical ionization rate obtained by Yablonovitch and Bloembergen subsequently became one of the main arguments in favor of the avalanche model.[11,12]

The frequency dependence of E_B enters this clas-

sical avalanche theory through the rate at which conduction electrons gain energy via inverse bremsstrahlung as well as through the probability for the electron energy to reach the ionization limit. The former can be shown to be related to the dc breakdown field via[8]

$$E_B = E_B(\mathrm{dc})(1+\omega^2\tau_c^2)^{1/2}. \quad (2)$$

Since in alkali halides $\tau_c \leq 10^{-15}$ sec, one expects very little change of E_B up to the ruby frequency, again in apparent agreement with recent experimental observations.[10,12] Thus, by using $W_i(E)$ from dc data and by independently extracting the ω dependence of E_B from Eq. (2), the avalanche model apparently provided a suitable description of dielectric breakdown in alkali halides at optical frequencies ω up to about 10^{15} sec^{-1}.

The dependence of E_B on frequency, which one obtains in NaCl on closer examination of the probability for free electrons to be accelerated to the ionization limit in a sequence of electron-photon-phonon collisions is, however, characterized by a rapid decrease with increasing ω. Therefore, as Sparks pointed out, avalanche formation by that mechanism in NaCl may well be impossible at optical or near-ir frequencies.[4] An electron will, on the average, just oscillate in an ac field rather than continuously gain energy unless it suffers backscattering collisions during the short time interval in which the E vector changes direction. The very same electron which has accelerated with the aid of such a backscattering collision must repeat this process until its energy is sufficient to generate a second one by impact ionization. Such a sequence of reversing collisions is so unlikely at optical frequencies[4] that the theory has been appropriately named "lucky reversing electron theory."[13-15]

The lucky electron theory was thought to be the logical explanation for the observed statistical nature of damage by Q-switched lasers[16,17]; since the interval between the start of the laser pulse and the initiation of avalanche by at least one "lucky electron" will not be constant, the avalanche may or may not have sufficient time left during the remaining duration of the pulse to reach breakdown proportions. Thus, for constant laser peak power and otherwise identical experimental conditions, some shots will result in damage and others will not. Recently, however, experimental artifacts and several prebreakdown material modifications have been shown to be responsible for some features of the observed laser damage statistics.[18-20] Careful experimentation does indeed yield a distinct threshold behavior of the breakdown field strength.[11,12] Therefore, at the present time, it appears that the lucky electron theory is not valid for optical breakdown.

Sparks[4] introduced the Holstein process and various vertical intraconduction-band transitions to amend the avalanche idea at optical frequencies. These processes let the electron absorb a quantum $\hbar\omega$ with reasonably high probability that it may reach the ionization limit in one or more Holstein steps or intraconduction-band transitions or combinations of both. This theory, while still in a very preliminary state, appears to explain the main features of avalanche breakdown at photon frequencies up to the far uv, although its prediction of breakdown field frequency dependence has recently been shown by Smith *et al.*[12] to contradict experimental findings.

A fundamental concept, first pointed out by Hellwarth,[21] was widely overlooked during the debate about the physical processes involved in breakdown. Instead of concentrating on how a few fortunate "hot" electrons may be generated during the interaction, he suggested that attention be focused on all the other electrons that absorb energy: which energy, being insufficient for impact ionization, is nevertheless dumped into the lattice. The resulting increase in temperature may cause irreversible lattice modifications (breakdown) before the onset of an avalanche. The absorbed energy can be transferred by the photocarriers via Joule heating of the lattice in a time much shorter than the laser pulse length. This notion of almost instantaneous energy deposition into the lattice seems particularly persuasive in view of the fact that electrons in ionic crystals interact strongly with the lattice via the electrostatic coupling.

In the present paper, the Hellwarth picture of optical breakdown in dielectrics is adopted in an attempt to compare its features with experimental laser breakdown data as a function of laser frequency and pulse length for representative alkali halides. An important aspect of such a breakdown model is the generation of a sufficient density of charge carriers, in the absence of impact ionization. Single- and multiphoton photocarrier generation are obvious mechanisms. The present theory can therefore be viewed as an attempt to deal with multiphoton absorption as a damage mechanism as was first suggested by Bloembergen.[6] Without going into specific detail, he argued that at laser frequencies $\omega \sim E_g/2\hbar$ (E_g is the band-gap energy), multiphoton absorption, instead of just providing starting electrons for the avalanche,[10] begins to dominate impact ionization as the more effective mechanism for charge carrier production. In this context the frequency dependence of the multiphoton breakdown theory presented in this paper is of particular interest. According to Bloembergen and his co-workers,[12] we

should expect it to fail for $\omega < E_g/2\hbar$ or, in other words, whenever a multiphoton process of order $N > 2$ is required for the transition across the forbidden gap. In the following, we will attempt to test this expectation for order $N = 2$ up to the order $N = 8$ required for band-to-band transitions in NaCl at the Nd wavelength.

The criteria for breakdown are not well defined. However, it has proven quite useful to assume that breakdown occurs as soon as the material melting point has been reached.[3] We maintain this criterion for the following discussion in which laser breakdown of dielectrics is treated on the basis of multiphoton-generated charge carriers which, "dressed" as polarons (instead of as free carriers as before), absorb energy from the field and heat the lattice. Such a system of electrons coupled electrostatically to the lattice and moving under an external field together with their induced lattice distortion is well known from polaron theory.

II. MULTIPHOTON POLARON ABSORPTION MECHANISM

The theory of laser-induced damage presented here is based on (i) polaron generation via single- or multiphoton absorption whereby valence electrons are excited into the conduction band and (ii) single- or multiphoton absorption in polaron-photon-phonon collision processes. This approach differs from the one used by Sparks[4] mainly in not requiring that the electrons be accelerated to the ionization limit. *A priori*, therefore, avalanche is ruled out and damage is assumed to occur only by polaron Joule heating. As stated before, the incentive for such an investigation was given by the difficulties in explaining avalanche at photon frequencies in the visible and the realization that, with increasing photon energy, multiphoton photocarrier generation is expected to somehow take over as the dominant breakdown mechanism.[6]

The analytical formalism we use is a set of differential equations for the concentration of polarons and for the lattice temperature. The required multiphoton cross sections $\sigma^{(M)}$ for carrier generation are taken from the literature. Though well known for lower orders, the cross sections for higher orders are uncertain. We will try to take account of this fact by discussing results obtained for a range of cross sections. The absorption coefficient K, for photons in the polaron-photon-phonon collision process, which in turn is responsible for the temperature increase, requires some further discussion.

The computational methods employed to obtain K were originally derived by Feynman *et al.*,[22] to calculate the mobility of low-energy electrons in polar crystals. This method has proven very powerful for all problems in which moving electrons interact simultaneously with many phonons such that the individual collisions cannot be separated in time. Based on a path-integral method,[22] the polaron conductivity tensor with[23] and without[24] a magnetic field present, the optical absorption of polarons,[25] and the polaron conductivity tensor in the presence of an intense laser field have all been studied. Recently Pokatilov and Fomin[26] applied this technique to the problem of multiphoton absorption by polarons for different types of interaction mechanisms between the polaron and the surrounding lattice. With the variables V and μ defined by the respective electron-phonon scattering mechanism they arrive at the following expression for the N-photon polaron absorption coefficient as a function of the local laser field strength E:

$$K_N = \frac{2\pi N n_c}{F(t)\hbar}\left(\frac{2\pi m}{k_B T}\right)^{1/2}\sinh(aN)\left(\frac{\hbar}{2m\omega}\right)^{\mu-1}\frac{V(0.5\beta)^N}{(N!)^2(2N+1)}\sum_{P=0}^{\infty}\frac{(-1)^P(2\beta)^P(0.5+N)^2{}_P}{(P!)(1+N)_P(1+2N)_P(1.5+N)_P}$$
$$\times\{(N+\xi)^{-\mu+N+P+1}K_{-\mu+N+P+1}[a(N+\xi)] + |N-\xi|^{-\mu+N+P+1}K_{-\mu+N+P+1}[a|N-\xi|]\}, \quad (3)$$

where $a = \hbar\omega/k_B T$, $\beta = e^2E^2/2m\hbar\omega^3$, $K_\nu[\ ]$ is the MacDonald function, $\hbar\omega$ the laser photon energy, m the polaron mass, k_B the Boltzmann constant, n_c the polaron density, $\hbar\omega_0$ the respective phonon energy, and $\xi = \omega_0/\omega$. For acoustical-phonon scattering, $\mu = 0$ and $V = k_B T \mathcal{E}_1^2/4\pi^3\hbar u_s^2\rho$, while for optical-phonon scattering, $\mu = 1$ and

$$V = \frac{\alpha(\hbar\omega_0)^{3/2}}{\pi^2(2m)^{1/2}\sinh(\hbar\omega_0/2k_B T)}.$$

Here u_s is the speed of sound, α the optical coupling constant, ρ the mass density, and $\mathcal{E}_1$ the deformation-potential constant. The total absorption coefficient K is given by

$$K = \sum_{N=1}^{\infty} K_N.$$

The method used to obtain Eq. (3) contains several simplifications. Firstly, the electrons' disper-

sion is assumed quadratic. Secondly, the interaction between electrons and lattice vibration modes is such that only one particular mode (either the optical or the acoustical) is selected in each instance and, for the chosen mode, dispersion is neglected. Furthermore, all parameters are considered temperature independent. In the case of optical-phonon scattering the coupling constant α is chosen to represent weak or intermediate coupling. Thirdly, no crystallographic anisotropy is taken into account and the laser field is assumed linearly polarized. Consequently, with all these assumptions, the calculations presented below are not expected to exactly reproduce observed breakdown data. However, we do expect them to indicate trends and provide long-wavelength limits for the validity of the multiphoton-polaron mechanism.

The variables n_c and T in Eq. (3) are obtained from the appropriately modified differential equations used in our previous breakdown studies.[3] As before, the change in conduction carrier density n_c as a function of photon flux F (and of time for pulsed laser fields) is assumed to result from multiphoton carrier generation:

$$n_c(t) = n_v(0)\left[1 - \exp\left(-\sigma^{(M)}\int_0^t F^M(t')dt'\right)\right], \quad (4)$$

where M is the order of the multiphoton process, $\sigma^{(M)}$ the generalized cross section, and $n_v(0)$ the density of valence electrons in a given material at time $t=0$. The laser pulse shape is assumed to be $F(t) = A^* \sin^2(\pi t/t_p)$. A^* is the peak flux and t_p the total pulse duration.

The increase in temperature T is calculated from

$$\frac{dT}{dt} = \frac{FK\hbar\omega}{c_0\rho}, \quad (5)$$

where c_0 is the specific heat of the dielectric.

For the acoustical- and optical-phonon scattering modes it is necessary to correct for the change in the refractive index as a function of polaron density when calculating K and converting optical fluxes into rms field strengths. In the case of optical phonons the phonon contribution to the polaron part of the permittivity as opposed to the pure lattice part has been analyzed by Gurevich *et al.*[27] in the limit of small α, resulting in the relation

$$\epsilon_p(\omega) \equiv \epsilon_{p1} + i\epsilon_{p2} = 4\pi i\sigma(\omega)/\omega, \quad (6)$$

where $\sigma(\omega)$ is the conductivity. In this case the real part of the conductivity becomes, for $\hbar(\omega - \omega_0) \gg k_B T$,

$$\mathrm{Re}\sigma(\omega) = \frac{2n_c e^2\alpha}{3m\omega_0}\left(\frac{\omega_0}{\omega}\right)^{5/2}\left(1 - \frac{\omega_0}{\omega}\right)^{1/2}. \quad (7)$$

Following similar procedures and replacing the matrix element for free-electron–optical-phonon interaction by that for the deformation potential for free-electron–acoustic-phonon interaction[28]

$$|C_q|^2 = \mathcal{E}_1^2 k_B T/2qVu_s^2,$$

(V is here an integration volume), we arrive at the following relation again, with $\hbar(\omega - \omega_0) \gg k_B T$:

$$\mathrm{Re}\sigma(\omega) = \frac{e^2\mathcal{E}_1^2(k_B T)^{1/2}m^{1/2}n_c}{\hbar^3\pi^{3/2}\omega\rho u_s^2}\left(1 - \frac{\omega_0}{\omega}\right)^2 \times\left[\exp\left(\frac{\hbar\omega_0}{k_B T}\right) + 1\right]. \quad (8)$$

As has been explained already, our calculations presume the polarons not to acquire sufficient energy from the radiation field to enter into an energy range where the deformation-potential scattering occurs predominantly with zero-point lattice oscillations.[28] Thus, the real part of the conductivity as expressed by Eqs. (7) and (8) is valid over the whole energy range of interest here. An additional term $\mathrm{Im}\sigma(\omega)$, required to calculate the polaron permittivity, has been derived[27]:

$$\mathrm{Im}\sigma(\omega) = n_c e^2/m\omega. \quad (9)$$

The total permittivity can be separated into the polaron portion and the lattice portion:

$$\epsilon(\omega) \equiv \epsilon_p(\omega) + \epsilon_L(\omega) \equiv \epsilon_I + i\epsilon_{II}, \quad (10)$$

with

$$\epsilon_L(\omega) = \epsilon_\infty\frac{\omega_l^2 - \omega^2 - i\omega\gamma}{\omega_t^2 - \omega^2 - i\omega\gamma} \quad (11)$$

(ω_l and ω_t represent longitudinal and transverse optical vibration frequencies, and γ acts as a damping parameter for optical vibrations and was considered negligibly small in our calculations, $\gamma \ll \omega_t$). Substituting Eq. (7) or Eqs. (8) and (9) in Eqs. (6) and (10), one easily derives the real and imaginary parts of the total permittivity and in turn the linear refractive index n_0, defined by

$$n_0 = \tfrac{1}{2}[\epsilon_I + (\epsilon_I^2 + \epsilon_{II}^2)^{1/2}]^{1/2}. \quad (12)$$

To allow for the response of the nonlinear lattice polarization to very intense fields the nonlinear refractive index n_2 is included as well. Thus the total refractive index n is given by

$$n = n_0 + n_2 E^2, \quad (13)$$

and n_0 is identical with the usual linear refractive index in the absence of free carriers.

Having obtained all the necessary formalism, we will now proceed to study breakdown fluxes for different laser wavelengths and pulse durations. From our previous calculations we retain the temporal laser pulse shape as $F = A^* \sin^2(\pi t/t_p)$, with F being the momentary and A^* the peak photon flux and t_p the total pulse length.[3,18,19] Further-

more, we retain the condition that breakdown occurs at a time $\frac{1}{2}t_p$ when the local temperature at that time is the melting point of the material under study. These conditions have been discussed at length.[3] The polaron density $n_c = 0$ at $t = 0$ and $T = 300$ K.

It is intuitively satisfying to study breakdown within two limits: (i) the polaron should be allowed to absorb just as many photons as necessary to gain energy sufficient for cascade ionization, thus allowing for "hot" polarons, and (ii) the polaron absorption mechanism should be limited to "low-order multiphoton absorption" so as to avoid impact ionization. Either one of these pictures will provide a criterion for determining whether an avalanche assumption in optical breakdown is indispensable at all or only for a limited frequency range. In effect, this distinction within one model either stresses the existence and necessity of "hot" carriers on the one hand, or concentrates solely on the contribution of all the other carriers to produce breakdown on the other. However, calculations of a complete polaron avalanche pose a serious problem, since no cascade ionization rates or cross sections consistent with the present formalism are known up to now. Results presented in the following apply therefore only to the "low-order multiphoton absorption" limit. The question of what constitutes "low order" was decided by requiring that our results (breakdown fluxes at $\frac{1}{2}t_p$) maintain a precision of about 1% for consecutive stepwise increases in the order of polaron multiphoton absorption. In all examined cases of both scattering mechanisms for different wavelengths and laser pulse lengths only $N = 1$ contributed to K with sufficient precision. As a consequence, *all our results represent damage events due to single-photon absorption by polarons and instantaneous energy transfer to the lattice.*

IV. RESULTS AND DISCUSSION

A. Beam deformation

The purpose of this section is to briefly discuss the present calculations in the light of very recent experiments on optical-breakdown morphology in alkali halides, as well as to establish a link between the formalism at hand and the problems of beam deformation via self-focusing and self-defocusing. Actual breakdown experiments inevitably are difficult to perform and to interpret because of the intricate role beam deformation plays in determining the effective local breakdown field strength. Measured breakdown field strengths normally must be corrected for self-focusing,[10-12] which results from the increase in refractive index due to the nonlinear term n_2E^2. Yablonovitch and Bloembergen,[7] however, have pointed out that this local increase in refractive index can be counterbalanced by a decrease due to the presence of an increasing number of free carriers. These may be generated either by an avalanche or by other mechanisms. In principle, then, corrections to measured breakdown fields should take into account both contributions to the refractive index. However, the actual density of free carriers at breakdown has never been measured in optical-breakdown experiments. The time evolution and the value at breakdown of the decreasing part of the refractive index are in general unknown. It might be for this reason that self-focusing corrections to breakdown data have attracted far greater attention than self-defocusing corrections. The latter are nevertheless required because of the sharp increase in the free carrier concentration prior to and at breakdown. Calculations of the refractive index based on Eqs. (12) and (13) show, for different laser wavelengths and pulse lengths, a consistent slight increase in total refractive index during the early stages of a damaging pulse. This is followed by a sharp decrease, still early in the pulse, once the photon flux is sufficiently high to efficiently pump carriers from the valence band via the respective multiphoton absorption processes.

Figure 1 illustrates a typical case of this behavior for NaCl for a 30-psec ruby pulse. In this figure as in all other figures presented herein, calculations were performed for the acoustical-phonon scattering mechanism using the parameters listed in Table I. Breakdown occurs at the center of the pulse (15 psec) with a flux of 8.4×10^{29} photons/cm^2 sec. Obviously, the onset of drastic changes in the local refractive index occurs far below these breakdown fluxes (see inset). However, the density of absorbing polarons monotonically increases up to breakdown. As a result, the competing effect of n_2 is completely overpowered above a certain threshold field strength, in agreement with earlier expectations.[7] In view of this result the contribution of polarons to the total local refractive index within the breakdown volume cannot be neglected, and local field corrections to breakdown data cannot be limited to self-focusing alone. One must deal with beam deformation caused by initial self-focusing, followed by defocusing as soon as the free carrier density is large enough ($\sim 10^{16}$ cm^{-3}).

Consider a laser beam, having a peak flux F just sufficient to damage at $\frac{1}{2}t_p$, being focused into a dielectric. Early in the pulse the focal waist will be reduced in diameter owing to the dominance of n_2E^2 over the negative free carrier contribution n_p to the total refractive index. As soon as the free-carrier density exceeds about 10^{16} cm^{-3}, defocusing will

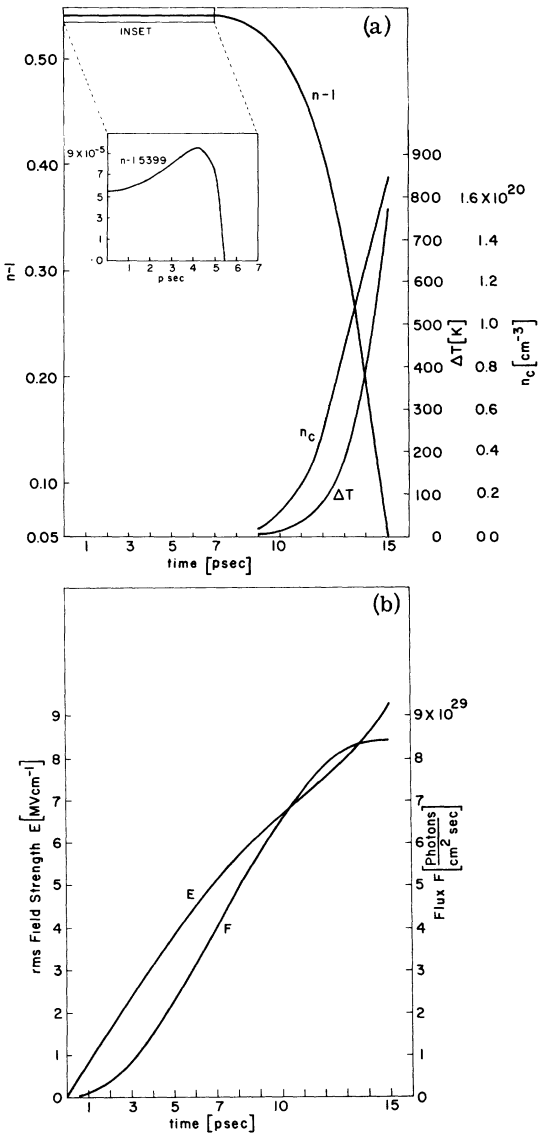

FIG. 1. (a) Time evolution of the refractive index n, the density of polarons n_c, and the temperature $\Delta T = T - 300$ K during a 30-psec laser pulse of the form $F = 8.4\times10^{29}\sin^2(\pi t/t_p)$ (photons cm^{-2} sec^{-1}) for which breakdown occurs at $t = \frac{1}{2}t_p = 15$ psec. The inset shows details of the initial increase of the refractive index due to the nonlinear refractive index n_2. (b) Time evolution of the photon flux F and the local rms field strength E under the same conditions as in (a). The breakdown field strength is $E_B = E(\frac{1}{2}t_p) = 9.2$ MV cm^{-1}. These and all subsequent figures are based on calculations using the acoustical-phonon-scattering mechanism in NaCl for which the parameters are listed in Table I.

occur because now $|n_p| > n_2E^2$. This in turn will reduce F and, therefore, n_c just behind the location of this initial focal waist reduction. At some point, n_c will again be small enough to make self-focusing possible, leading to increased concentrations n_c and, as a consequence, to self-defocusing, etc. Thus, one can speculate that, owing to the interplay of the two competing beam-forming mechanisms, a spatially periodic sequence of zones with alternating high magnitudes in carrier densities is generated. Extending this speculation a bit further, it may well be that the breakdown morphology observed for peak powers just above the laser damage threshold is a manifestation of periodic changes in total n_c.[12]

B. Acoustical-phonon scattering

For the reason discussed in the previous section, local breakdown fields are meaningful only if corrections for the nonlinear refractive index as well as those for the breakdown carrier density are considered. We therefore will abandon the custom of investigating breakdown fields as a function of laser pulse length in favor of local breakdown photon fluxes. This does not rule out estimations of properly corrected breakdown fields. In order to determine the value of local breakdown fields corresponding to our breakdown fluxes, we first calculate the effect of polarons on the local refractive index and convert, in a subsequent step, the photon fluxes to rms field strengths by making use of this local refractive index. Thus, we ascertain a master-slave relationship between the driving photon flux which can be measured experimentally and the induced local rms electric field which is experimentally inaccessible. If under certain conditions, as will be shown below, e.g., in the nanosecond regime, the polaron density at breakdown does not exceed 10^{19} cm^{-3}, its influence on the total refractive index remains minor and a comparison between experimentally found breakdown fields and the ones estimated here will be possible. Note in passing that this polaron density agrees well with the 10^{18}-cm^{-3} electrons chosen in earlier laser breakdown work as a damage criterion[10] for nanosecond pulses as well as with pre-breakdown electron density measurements in borosilicate crown glass (BSC-2).[29] This situation changes drastically in the picosecond regime where polaron densities larger by two orders of magnitude are calculated at the time of breakdown. Again, a similarly high density in free carriers has been shown[3] to be necessary for avalanche breakdown, although later experimental determinations of picosecond breakdown fields have not taken into account the consequences resulting from it.[11,12] Thus, a comparison of the present results with experimental data remains confined to the nanosecond regime. We shall demonstrate the importance of this distinction between breakdown field and flux by plotting for a 30-psec pulse the

TABLE I. Parameters for NaCl.

Symbol	Meaning	Value	Multiphoton cross sections $\sigma^{(M)}$ ($cm^{2M}\,sec^{M-1}$)	
ρ	mass density	2.165 g cm^{-3} [a]	$\sigma^{(2)} = 4 \times 10^{-49}$ [h]	
c_0	specific heat	2.0 cal $g^{-1}K^{-1}$ [b]	$\sigma^{(3)} = 1 \times 10^{-80}$ [i]	
α	coupling constant	3.50	$\sigma^{(4)} = 1.45 \times 10^{-111}$ [h]	
ϵ_∞	high-frequency permittivity	2.35 [c]	$\sigma^{(5)} = 5 \times 10^{-141}$ [j]	
ϵ_0	static permittivity	5.62 [c]	$\sigma^{(8)} = 1.5 \times 10^{-225}$	
$\hbar\omega_l$	longitudinal optical phonon	3.25×10^{-2} eV [d]		
$\hbar\omega_t$	transverse optical phonon	2.05×10^{-2} eV [e]		
$\hbar\omega_0$	longitudinal acoustic phonon	1.61×10^{-2} eV [e]		Initial refractive
u_s	velocity of sound	4.67×10^5 cm sec^{-1} [a]	λ (μm)	index n_0 [k]
m	polaron mass	$0.75m_e$ (free mass)		
$\mathcal{E}_1$	deformation-potential constant	8.9 eV	1.0642	1.53
n_2	nonlinear refractive index	6.4×10^{-13} esu [f]	0.6943	1.54
n_v	initial valence electron density	2.24×10^{22} cm^{-3}	0.5321	1.55
T_M	melting point	1074 K	0.3471	1.58
E_g	band-gap energy	8.6 eV [g]	0.1720	1.90

[a] From Ref. 34.
[b] From *Handbook of Chemistry and Physics* (Chemical Rubber Co., Cleveland, 1973).
[c] See Ref. 35.
[d] See Ref. 36.
[e] See Ref. 37.
[f] From Ref. 11.
[g] From Ref. 33.
[h] See Ref. 38.
[i] See Ref. 39.
[j] From Ref. 31.
[k] See Ref. 40.

local refractive index and the local rms field as a function of time up to breakdown at $\frac{1}{2}t_p$. Figure 1 shows an initial increase of n due to the absence of any free carriers or polarons simply as a result of the additive effect of the nonlinear term n_2E^2. The importance of this increase to self-focusing is evident. We note, however, that with increasing flux and, as a consequence, with increasing probability for band-to-band excitation the population of the conduction band begins first to counterbalance and later to completely overpower this positive contribution to the refractive index. As can also be seen in Fig. 1, this occurs early in the damaging pulse. Once the refractive index has started to dwindle, there is no reason to expect a reversal trend before breakdown, since both the photon flux and the band-to-band excitations continue to increase monotonically. The rapidly falling refractive index then forces the local electric field up according to $E \propto n^{-1/2}$. Therefore, the rms field strength at breakdown depends on the refractive index and the number of polarons necessary for breakdown at a particular laser wavelength and pulse length. Without knowledge of this polaron density the exact value of the local breakdown field strength cannot be determined.

After having established that the polaron density is a crucial quantity in optical breakdown, the polaron generation rate attains significance as well. Cross sections for multiphoton band-to-band excitation, particularly those of higher orders, are not widely investigated in solids. The present calculations attempt to accommodate this fact by using a range of plausible cross sections. However, all cross sections used here (Table I) are the smallest published in the literature, with the exception of that for Nd photons. In this case, an eight-photon process is necessary to bridge the band gap of NaCl. No values for $\sigma^{(8)}$ in solids are available from the literature, and therefore a trial cross section was taken from multiphoton ionization experiments on Kr.[30] This value was arbitrarily modified so that a reasonable value of E_B was obtained for a 30-nsec pulse and this cross section was used henceforth. In case of the ruby frequency, reasonable agreement with measured data[10,14] for nanosecond laser pulses was obtained with the cross section $\sigma^{(5)} = 5 \times 10^{-141}$ used in previous calculations.[3] In order to demonstrate the dependence of the breakdown parameters on this cross section we also arbitrarily increased its value by one order of magnitude (Table I). This was also done for the doubled frequency of ruby. As we will see later, the cross sections significantly control general breakdown behavior and, as one would expect, are crucial in the present theory. The remaining parameters employed in the breakdown flux calculations, e.g., acoustical-phonon frequency and deformation-potential constant, are listed in Table I as well.

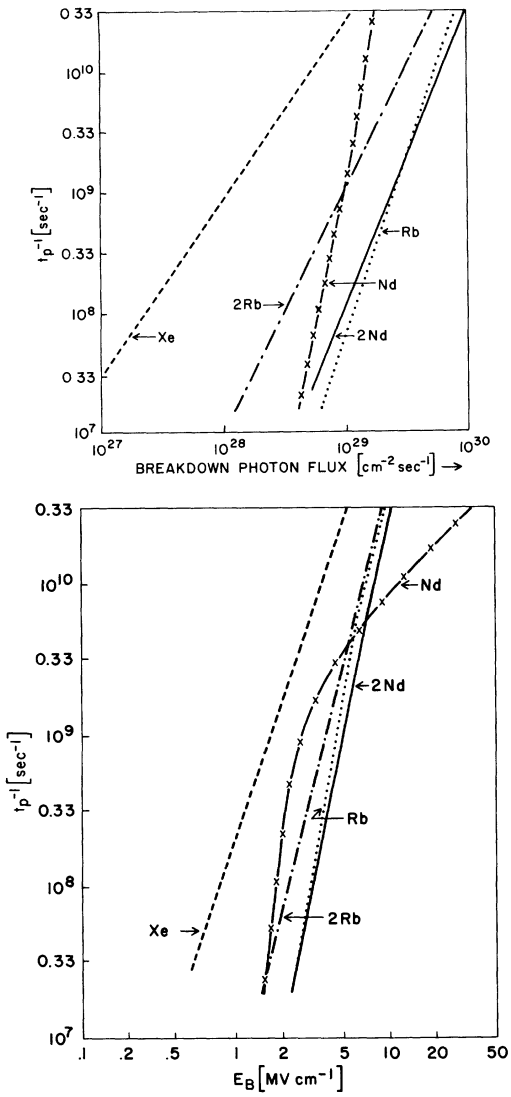

FIG. 2. (a) Breakdown photon flux A_B^* in NaCl vs inverse laser pulse length. t_p^{-1} calculated for different laser frequencies: Nd, neodymium laser frequency; 2Nd, doubled frequency of neodymium laser; Rb, ruby laser frequency; 2Rb, doubled frequency of ruby laser; Xe, xenon laser frequency. (b) Breakdown field strengths E_B under the same conditions as in (a).

In Fig. 2(a) we display breakdown fluxes A_B^* as a function of inverse pulse length for various laser frequencies. We observe a straight-line dependence on a double logarithmic scale. Indeed, the relation $t_p^{-1} \propto (A_B^*)^{(M+1)/2}$ is easily derived from Eqs. (4) and (5). In Fig. 2(b), we display the breakdown field strength E_B as a function of the reciprocal pulse length, in order to illustrate the effect of the changing refractive index on the conversion of flux to field strength.

If one rearranges the calculated data as in Fig. 3, such that for a set of identical pulse lengths the breakdown flux is plotted against the photon energy, a breakdown frequency dependence appears which qualitatively resembles the frequency dependence expected from the avalanche model in the region between the Nd and double Nd laser frequencies. Note that lack of a considerable frequency dependence in this range seems to rule out multiphoton processes as the dominant mode of optical breakdown in dielectrics.[11,12] By exclusively considering the vast difference in cross sections (see Table I) one would expect a steep decline in breakdown fluxes with increasing laser frequency if multiphoton processes were to play a significant role. This decline was never observed experimentally, nor is it corroborated by our present calculations.

In Fig. 4 we compare experimental breakdown field strengths for a $t_p = 60$ nsec pulse[10] with our wavelength-dependent data. Unfortunately, other published experimental data[11,12] down to 0.34 μm cannot be strictly compared for reasons stated above. As is evident from Figs. 3 and 4, damage field thresholds decrease markedly only for laser photon energies larger than 3 eV in NaCl. However, the decrease is not as dramatic as expected solely on the basis of multiphoton band-to-band excitation cross sections. The reason for that becomes evident upon examination of the normalized

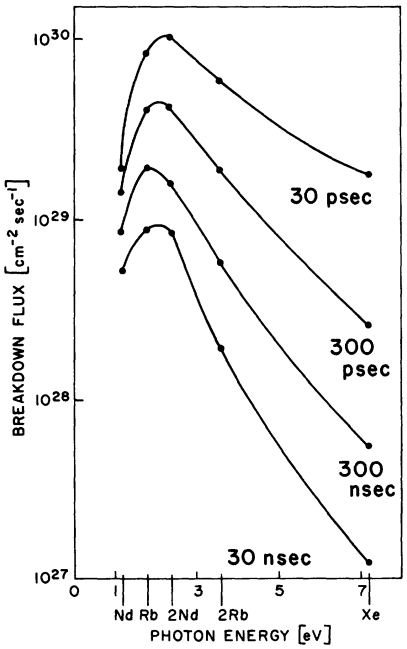

FIG. 3. Breakdown flux A_B^* in NaCl vs the energy of the laser photons for different pulse length t_p.

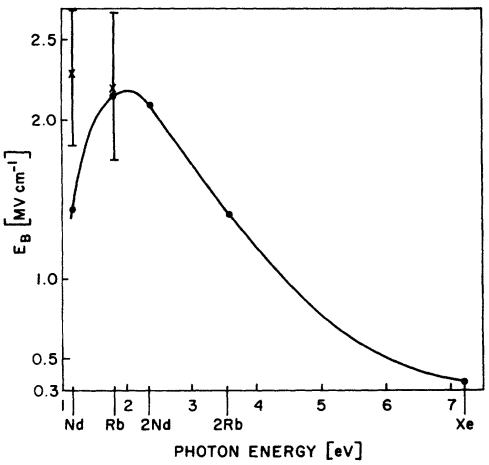

FIG. 4. Breakdown field strength E_B in NaCl vs photon energy for a $t_p = 60$ nsec pulse. Experimental data from Ref. 10.

polaron absorption coefficient and its wavelength dependence. This is shown in Fig. 5, where the ratio of K/n_c is plotted versus laser photon energy at breakdown. In effect, the influence of increasing probability for free carrier generation with increasing photon energy on the breakdown flux is weakened by a sharp decrease in the polaron absorption coefficient.

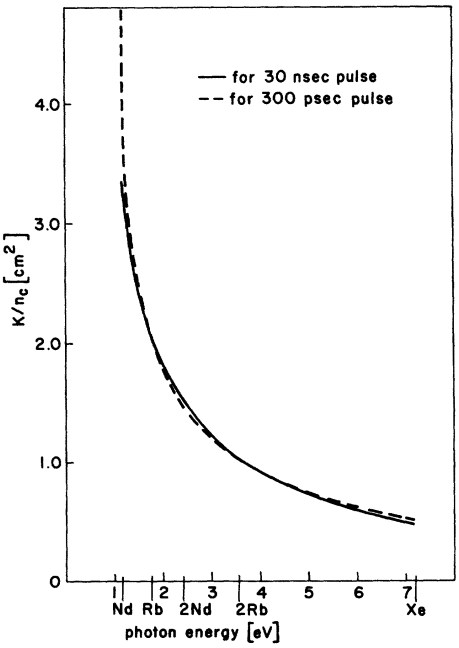

FIG. 5. Polaron photon absorption coefficient K divided by polaron density n_c in NaCl at breakdown ($t = \frac{1}{2}t_p$) vs photon energy for a 30-nsec and a 300-psec pulse. K/n_c in units of 10^{-17} (cm^2).

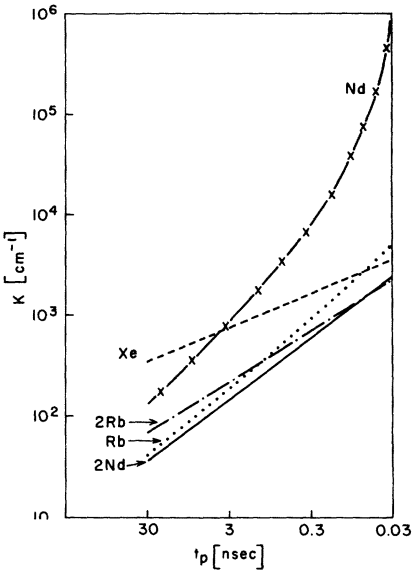

FIG. 6. Polaron photon absorption coefficient K of NaCl at breakdown ($t = \frac{1}{2}t_p$) vs laser pulse length for different laser photon energies.

The calculated polaron absorption coefficient at breakdown as a function of pulse length and wavelength is illustrated in Fig. 6. Of particular interest at this point is the large absorption coefficient at breakdown for a 30-psec Nd pulse. It should be possible to observe beam depletion by polaron absorption in this particular case at peak powers at or slightly below breakdown. Such an experiment would test the validity of the polaron optical-breakdown model at the Nd frequency. On the other hand, it seems very unlikely to observe beam depletion in commonly found experimental arrangements (tightly focused beams) for all the other frequencies discussed here.

Beam depletion or attenuation should be considered carefully. Two mechanisms are responsible: (i) the removal of photons due to carrier generation and (ii) photon absorption by the generated carriers in heating the lattice. Let us consider first the former, which is simply a consequence of the creation of a large density of charge carriers. This density assumes its highest value right at the moment of damage and, as previous calculations have shown,[3] this peak density increases from around 10^{18} cm^{-3} for nanosecond pulses to over 10^{20} cm^{-3} for picosecond pulses. Thus we expect that beam depletion, if it exists, will be most pronounced for extremely short pulses. Attenuation due to charge carrier generation may be characterized by an absorption coefficient $\alpha(A_B^*)$ at $\frac{1}{2}t_p$ of a just damaging pulse: for pure avalanche,

$$\alpha_A(A_B^*) \geq E_g n_c W_i(A_B^*)/F\hbar\omega;$$

for multiphoton polaron generation,

$$\alpha_M(A_B^*) = \sigma^{(M)} A_B^{*M-1} n_v .$$

Some simple calculations show that $\alpha(A)$ may indeed reach large values. Consider a 15-psec full width at half maximum (FWHM) Nd-laser pulse. For pure avalanche breakdown, according to calculations by Kelly *et al.*,[19] $A_B^* = 10^{31}$ photons cm^{-2} sec^{-1} at the damage threshold, and $n_c = 1.3 \times 10^{20}$ cm^{-3}. For this case $W_i(A_B^*) = 10^{12}$ sec^{-1} is obtained from the work of Fradin and co-workers.[9,10] The resulting value for the free carrier generation absorption coefficient is $\alpha_A \approx 110$ cm^{-1}.

Another example is multiphoton polaron generation at the ruby frequency for the same 15-psec FWHM pulse. With[31] $\sigma^{(5)} n_v = 1.12 \times 10^{-118}$ cm^{10} sec^4 and $A_B^* = 1.44 \times 10^{30}$, for which damage occurs again at $\frac{1}{2}t_p$, we obtain $\alpha_5 \approx 75$ cm^{-1}. Remembering that $\sigma^{(5)}$ is known only within an order of magnitude, we have again obtained an absorption coefficient for this case that is comparable to α_A.

This peak absorption coefficient increases with decreasing order of the multiphoton excitation process somewhat, but even for a three-photon process it remains at values comparable to those above. On first sight, then, beam attenuation due to charge carrier generation alone appears to be a real problem in the picosecond regime, irrespective of the damage mechanism. Note that the energy absorbed in this process remains almost completely in the crystal in the form of electronic excitation during the duration of the pulse. The excited states (electrons in the conduction band) relax during a time that is much larger than t_p via radiative and nonradiative transitions and thus do not contribute to lattice heating for $t \leq \frac{1}{2}t_p$.

Let us now turn briefly to the absorption coefficient associated with heating of the lattice. It is widely agreed[4] that energy transfer to the lattice from absorbing carriers happens via Joule heating. This can simply be expressed as the rate of increase of energy per unit volume[4]:

$$\frac{dW}{dt} = \sigma E^2 n_c = \frac{e^2}{m} \tau_c (1 + \omega^2 \tau_c^2)^{-1} E^2 n_c , \qquad (14)$$

where the conductivity σ is written in terms of parameters used previously in Eqs. (1) and (2). Balancing this energy density increase per unit time by the corresponding absorption term from the photon field,

$$\frac{dW}{dt} = \alpha_j F \hbar\omega , \qquad (15)$$

we arrive at an expression for the Joule heating absorption coefficient α_j:

$$\alpha_j = \frac{e^2}{m} \tau_c (1 + \omega^2 \tau_c^2)^{-1} n_c \frac{4\pi}{cn} \qquad (16)$$

(c is the speed of light, n the refractive index). As long as $\omega\tau_c$ is not very much larger than 1 and $\tau_c \leq 10^{-15}$ sec, we find at the damage threshold for a reasonable $n_c \sim 10^{20}$ cm^{-3} and $n \sim 1.5$ that

$$\alpha_j \leq 1.1 \times 10^4 \text{ cm}^{-1} .$$

As we can see from Fig. 6, with the exception of the 1.0642-μm line, the absorption coefficient K at breakdown consistently remains smaller than 10^4. In view of possible beam attenuation the comparison of absorption coefficients for (i) generation of carriers and (ii) heating of the lattice by those absorbers leads us to conclude that neither model—inverse-bremsstrahlung avalanche or multiphoton-generated polarons—will *a priori* prevent or enhance beam attenuation as argued previously.[12] We therefore do not believe that eventual beam attenuation will offer a means of distinguishing between the two models. The only time this might become possible would occur for very short pulses at the Nd frequency.

Figure 7 shows the refractive indices at breakdown for different frequencies as a function of pulse length. For a given laser frequency the refractive index decreases with decreasing pulse length owing to the increase in polaron density as shown in Fig. 8. We reemphasize in this connection the necessity to properly account for the changing refractive index when transforming laser fluxes to local rms electric field strengths. Obviously this becomes more important the larger the relative change, e.g., at the longer wavelengths, where most of the experiments have been performed up to now.

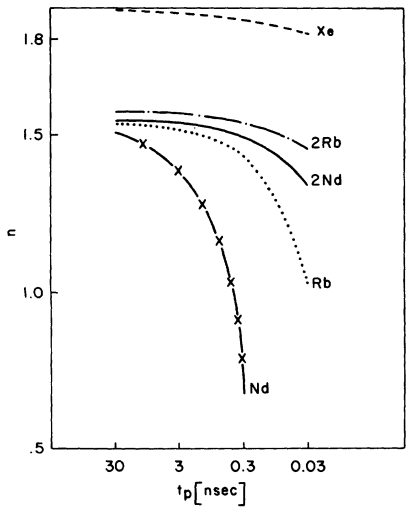

FIG. 7. Total refractive index of NaCl at breakdown ($t = \frac{1}{2}t_p$) vs laser pulse length for different laser photon energies.

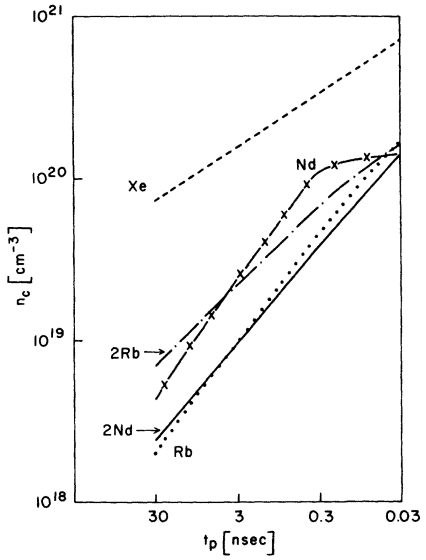

FIG. 8. Density of polarons in NaCl at breakdown ($t=\frac{1}{2}t_p$) vs laser pulse length for different laser photon energies.

Beam attenuation, self-focusing, and self-defocusing determine the local photon flux or the local rms field strength in a largely unknown and complicated fashion that has never been completely appreciated in experimental or theoretical laser breakdown work. For a pulse having a peak power right at the damage threshold we can conceive that damaging concentrations of charge carriers exist in a few very small zones of the self-focusing–self-defocusing pattern, located along the axis in the focal volume of the beam such that the total length of highly absorbing vestiges is very small (a few microns, as indicated by the damage morphology observed by Smith *et al.*[12]). Since the diameter of these areas is very small as well (e.g., a fraction of the beam waist diameter), rather small depletion of a beam with a flux that corresponds to the damage threshold will occur and then only at the maximum of the TEM_{00} laser intensity profile. This will remain largely unnoticed using conventional beam diagnostic techniques which measure the temporal pulse behavior and its total energy. Of course, right after damage occurs, the usual beam depletion is observed caused by hot plasma formation.[17]

C. Optical-phonon scattering

Since it is not immediately evident which of the two polaron-scattering mechanisms, the optical or acoustical, would result in breakdown data that are in better agreement with experimental ones, we recalculated all steps outlined in the previous section for the optical-scattering mechanism as well. The parameters used are also listed in Table I. It turned out that the polaron density at breakdown in the optical case is consistently higher, and breakdown under otherwise identical conditions occurs at significantly higher fluxes or local rms field strengths as compared to the acoustical case. We therefore believe that acoustical-phonon scattering dominates optical breakdown in dielectrics for the frequency range pertinent to this paper and that a future theory which allows for both phonon-scattering modes simultaneously would not yield results that are significantly different from those presented in the previous section.

D. Extension to NaBr

In Sec. IV B we discussed the pulse length dependence of the breakdown peak flux A_B^* and found it to obey the relation $t_p^{-1} \propto (A_B^*)^{(M+1)/2}$. We then tested the theory against the dependence of the breakdown field strengths on the laser frequency which were not found to decrease as rapidly as one would expect on first sight from a pure multiphoton mechanism. This behavior is in remarkable agreement with measured data for nanosecond pulses in the wavelength region $0.5321 \leq \lambda \leq 1.0642$ μm. These data had previously been taken as a strong indication for avalanche breakdown in NaCl and other alkali halides.

In this section we describe results of yet another test of our breakdown theory by considering materials other than Na Cl with the goal of investigating the influence of different band gaps on the breakdown flux. We chose again alkali halides for this comparison because in this way the effect of parameters such as specific heat, mass density, phonon energy, etc., other than the band gap will be minimized and because there are experimental data available in the nanosecond regime. Comparison with materials of different band gap is complicated by the uncertainties in high-order multiphoton absorption cross sections. As stated in Sec. IV B, the value of $\sigma^{(M)}$ is of considerable influence on the breakdown peak flux and, therefore, accurate values for A_B^* or E_B cannot be calculated. But not only are the cross sections fairly unreliable, but also exact band-gap data are not always available.

To reduce the $\sigma^{(M)}$ uncertainty somewhat, we chose NaBr, a material with a smaller band gap than that of NaCl. In this way, the multiphoton order M is lowered to 7 at the Nd wavelength and 4 at the ruby wavelength. An additional problem in this connection is, of course, the absolute value of the band gap, which is stated in the literature as low as 7.1 eV,[32] and as high as 7.7 eV.[33] The parameters used in the calculation of breakdown data

TABLE II. Values of the constants of NaBr used in the calculations.

Symbol	Meaning	Value
$\sigma^{(7)}$		4.64×10^{-197} cm^{14} sec^{6}
ρ	mass density	3.2 g cm^{-3}
c_0	specific heat	1.19 cal g^{-1} K^{-1}
ϵ_∞	high-frequency permittivity	2.64 [a]
ϵ_0	static permittivity	5.78 [a]
$\hbar\omega_l$	longitudinal optical phonon	2.7×10^{-2} eV [b]
$\hbar\omega_t$	transverse optical phonon	1.82×10^{-2} eV [a]
$\hbar\omega_0$	longitudinal acoustical phonon	1.57×10^{-2} eV [c]
u_s	velocity of sound	4.3×10^{5} cm sec^{-1}
m	polaron mass	$0.87 m_e$ (free mass)
$\mathcal{E}_1$	deformation-potential constant	7.92 eV
n_2	nonlinear refractive index	9.6×10^{-13} esu [d]
n_v	initial valence electron density	1.882×10^{22} cm^{-3}
T_M	melting point	1028 K
	Initial refractive index at 1.0642 μm = 1.62	
	Initial refractive index at 0.6943 μm = 1.63	

[a] See Ref. 35.
[b] See Ref. 36.
[c] See Ref. 41.
[d] See Ref. 12.

in NaBr are listed in Table II. Again, for the case of acoustical-phonon scattering, we find for ruby that the ratio $E_B(\text{NaBr})/E_B(\text{NaCl}) = 0.87$, which compares with the measured value[16] of 0.82. And then using the Nd ratio of 0.7 from experiment,[17] we obtain a reasonable value of $\sigma^{(7)}$ as shown in Table II.

E. Discussion of parameters

In order to investigate the influence on the calculated breakdown data of several parameters listed in Tables I and II, particularly of those whose values are known with less certainty, test runs were performed in which their values were changed. Aside from principle considerations, it is important to evaluate whether or not the agreement between computed results and experiments is merely fortuitous.

In the case of acoustical scattering the parameter least certain in value in alkali halides is the deformation-potential constant $\mathcal{E}_1$. In all initial calculations a value of $\mathcal{E}_1 = 8.9$ eV for NaCl was used which is close to the value of 9.95 eV suggested by Evseev and Tolpygo[34] for NaCl. Sparks[4] derived a value of 4.5 eV from the theory of monovalent metals. In view of this smaller value we performed all calculations with $3^{-1/2}\mathcal{E}_1$. The results are compared with the original results in Table III for a selection of representative pulse lengths. Breakdown fields consistently increase by around 20%, whereby the increase appears somewhat more pronounced for damage at the shorter wavelengths than in the red and ir. Altogether the changes solely due to $\mathcal{E}_1$ are not spectacular for any of the other breakdown variables, and one can safely assume that within the uncer-

TABLE III. Dependence of breakdown values for NaCl on choice of deformation-potential constant $\mathcal{E}_1$. For each wavelength values are given for $t_p = 30$ psec (top line) and $t = 30$ nsec (bottom line). The left column for each variable refers to $\mathcal{E}_1 = 8.9$ eV and the right column to $\mathcal{E}_1 = 8.9/\sqrt{3}$ eV.

λ (μm)	A_B^*		n_c		E_B		K	
1.0642	1.9×10^{29}	1.9×10^{29}	1.4×10^{20}	1.5×10^{20}	33.0	39.0	8.0×10^{5}	5.88×10^{5}
	5.1×10^{28}	5.8×10^{28}	4.3×10^{18}	1.1×10^{19}	1.54	1.66	1.4×10^{2}	1.23×10^{2}
0.6943	8.4×10^{29}	9.4×10^{29}	1.7×10^{20}	3.1×10^{20}	9.2	16.6	4.9×10^{3}	6.86×10^{3}
	8.7×10^{28}	1.0×10^{29}	2.0×10^{18}	5.1×10^{18}	2.47	2.71	4.1×10^{1}	3.41×10^{1}
0.5321	1.0×10^{30}	1.2×10^{30}	1.4×10^{20}	3.1×10^{20}	10.4	12.9	2.5×10^{3}	2.31×10^{3}
	6.5×10^{28}	8.1×10^{28}	2.4×10^{18}	5.8×10^{18}	2.44	2.77	3.7×10^{1}	2.97×10^{1}
0.3471	5.9×10^{29}	7.6×10^{29}	4.1×10^{18}	4.5×10^{20}	9.3	11.2	2.3×10^{3}	1.83×10^{3}
	1.9×10^{28}	2.5×10^{28}	6.9×10^{18}	1.6×10^{19}	1.6	1.84	7.0×10^{2}	5.29×10^{1}
0.1720	1.2×10^{29}	1.7×10^{29}	7.1×10^{20}	1.4×10^{21}	5.35	6.57	3.6×10^{3}	2.53×10^{3}
	1.2×10^{27}	1.7×10^{27}	1.3×10^{19}	1.5×10^{20}	0.53	0.63	3.5×10^{2}	2.44×10^{2}

tainty ranges still common to both experimental and theoretical work on laser damage, the present model suffers no serious deficiency because of lacking precision in $\mathcal{E}_1$.

As stated in Sec. II, one of the most serious simplifications of our model is neglect of phonon dispersion. It seems therefore indispensable to analyze to what extent the proper choice of phonon energy influences our breakdown results. Assuming that our averaged phonon energies were in error by ±20% for both cases, we recalculated all our results outlined in Sec. IV B.

For a 20% increase in phonon energy the largest relative change observed is a change of breakdown field of +7% for a 30-nsec pulse at 0.5321 μm and acoustical scattering. The largest relative change for a 20% decrease in phonon energy occurs for a 30-psec pulse at 0.5321 μm and acoustical scattering where the breakdown field decreases by almost 10%. This then is an indication of the accuracy of the calculated breakdown data presented here. Improvements are, of course, only possible by considering the phonon spectrum, and by exact knowledge of $\sigma^{(M)}$ as well as $\mathcal{E}_1$.

V. CONCLUSIONS

In conclusion, we find that optical dielectric breakdown at wavelengths between 1.06 and 0.172 μm can be explained quite successfully by the theory outlined above. This is achieved by assuming multiphoton band-to-band excitations to be the only charge-carrier-generation mechanism in NaCl and NaBr. Transfer of energy from the photon field to the lattice occurs exclusively via a polaron-photon absorption mechanism, whereby single-photon absorption by the polarons proves sufficient to explain NaCl measured breakdown behavior within a factor of 2. Thus, no lattice ionization process has to be involved. The concept of an electron avalanche damage started by a few hot electrons is replaced here by the concept of damage by many electrons, none of which has sufficient energy for lattice ionization but which collectively produce irreversible material changes.

We readily admit that many of the above considerations remain speculation as long as the breakdown event is not modeled in a complete space- and time-dependent manner. It should be appreciated that the breakdown model described herein cannot, in its present form, provide the necessary quantitative beam-forming and attenuation corrections. It simply assumes a local flux to be present irrespective of whether it is the result of self-focusing or any other beam-forming and attenuating mechanism. What in essence we have done, then, is to simply restrict the calculations to a crystal volume that was sufficiently small so as to neglect all these effects. We retained only the correction of the refractive index for the conversion of photon flux into rms optical field strength and vice versa.

As a consequence, direct comparison of presently available experimental and calculated breakdown data was somewhat problematic. Additional uncertainties arose from the fact that our model made use of a number of simplifying assumptions (see Sec. II); nevertheless, the polaron breakdown model appears to provide a genuine alternative to avalanche breakdown. In fact, the success of the present formalism, aside from indicating that the experimental determination of breakdown fields will have now to take into account the change in refractive index, also justifies its extension (i) to space- and time-dependent laser-beam profile analysis and (ii) to the CO_2 wavelength region. It is our intent to proceed in these areas and simply note in conclusion that the present work contains no reference to $\lambda > 1\mu$m because of the uncertainty in the multiphoton generation rates.

---

† Present address: Department of Physics, Washington State University, Pullman, Wash. 99164.

*Supported by U. S. ERDA under Contract No. E(45-1)-2221.

[1]G. M. Zverev, T. N. Mikhailova, V. A. Pashkov, and N. M. Soloveva, Zh. Eksp. Teor. Fiz. 53, 1849 (1967) [Sov. Phys. JETP 26, 1053 (1968)].

[2]L. H. Holway and D. W. Fradin, J. Appl. Phys. 46, 279 (1975).

[3]P. Bräunlich, A. Schmid, and P. Kelly, Appl. Phys. Lett. 26, 150 (1975).

[4]M. Sparks, ARPA Report No. DAHC 15-73-C-0127, 1975 (unpublished).

[5]Yu. P. Raizer, Usp. Fiz. Nauk 87, 29 (1965) [Sov. Phys. Usp. 8, 650 (1966)].

[6]N. Bloembergen, IEEE J. Quantum Electron. QE-10, 375 (1974).

[7]E. Yablonovitch and N. Bloembergen, Phys. Rev. Lett. 29, 907 (1972).

[8]E. Yablonovitch, Appl. Phys. Lett. 19, 495 (1971).

[9]D. W. Fradin, N. Bloembergen, and J. P. Lettelier, Appl. Phys. Lett. 22, 635 (1973).

[10]D. W. Fradin, Harvard University Technical Report No. 643, 1973 (ONR-372-0012) (unpublished).

[11]W. L. Smith, J. H. Bechtel, and N. Bloembergen, Phys. Rev. B 12, 706 (1975).

[12]W. L. Smith, J. H. Bechtel, and N. Bloembergen, Harvard University Technical Report No. 665, 1976 (ARPA F 44620-75-C-0088) (unpublished).

[13]M. Bass and H. H. Barrett, IEEE J. Quantum Electron. QE-8, 338 (1971).

[14]M. Bass and H. H. Barrett, Appl. Opt. 12, 690 (1973).

[15]M. Bass and D. W. Fradin, IEEE J. Quantum Electron. QE-9, 890 (1973).
[16]D. W. Fradin and M. Bass, Appl. Phys. Lett. 22, 206 (1973).
[17]D. W. Fradin, E. Yablonovitch, and M. Bass, Appl. Opt. 12, 700 (1973).
[18]N. L. Boling, P. Bräunlich, A. Schmid, and P. Kelly, Appl. Phys. Lett. 27, 191 (1975).
[19]P. Kelly, P. Bräunlich, and A. Schmid, Appl. Phys. Lett. 26, 223 (1975).
[20]D. Milam, R. A. Bradbury, and R. H. Picard, Natl. Bur. Stand. (U.S.) Spec. Publ. 435, 347 (1976).
[21]R. Hellwarth, Natl. Bur. Stand. (U.S.) Spec. Publ. 341, 67 (1970).
[22]R. P. Feynman, R. W. Hellwarth, C. K. Iddings, and P. M. Platzman, Phys. Rev. 127, 1004 (1962).
[23]A. A. Klyukanov and E. P. Pokatilov, Zh. Eksp. Teor. Fiz. 60, 312 (1971) [Sov. Phys.-JETP 33, 170 (1971)].
[24]N. I. Balmush, A. A. Klyukanov, and E. P. Pokatilov, Phys. Status Solidi B 67, 387 (1975).
[25]J. Devreese, J. DeSitter, and M. Goovaerts, Phys. Rev. B 5, 2367 (1972).
[26]E. P. Pokatilov and V. M. Fomin, Phys. Status Solidi B 73, 553 (1976).
[27]V. L. Gurevich, I. G. Lang, and Yu. A. Firsov, Fiz. Tverd. Tela (Leningrad) 4, 1252 (1962) [Sov. Phys.-Solid State 4, 918 (1962)].
[28]E. M. Conwell, Solid State Phys. Suppl. 9 (1967).
[29]N. Allyasini and J. H. Parks, Natl. Bur. Stand. (U.S.) Spec. Publ. 435, 356 (1976).
[30]A. Gold and H. B. Bebb, Phys. Rev. 143, 1 (1966).
[31]V. S. Dneprovskii, D. N. Klyshko, and A. N. Penin, JETP Lett. 3, 251 (1966).
[32]D. Fröhlich and B. Staginnus, Phys. Rev. Lett. 19, 496 (1967).
[33]S. Nakai and T. Sagawa, J. Phys. Soc. Jpn. 26, 1627 (1969).
[34]Z. Ya. Evseev and K. B. Tolpygo, Fiz. Tverd. Tela (Leningrad) 10, 1678 (1968) [Sov. Phys.-Solid State 10, 1325 (1968)].
[35]R. P. Lowndes and D. H. Martin, Proc. R. Soc. London Ser. A 308, 473 (1969).
[36]F. C. Brown, in *Polarons and Excitons*, edited by C. G. Kuper and G. D. Whitfield (Oliver and Boyd, London, 1962), p. 323.
[37]G. Raunio and S. Rolandson, Phys. Rev. B 2, 2098 (1970).
[38]A. Schmid, Ph.D. thesis, Technical University of Vienna, 1975 (unpublished).
[39]I. M. Catalano, A. Cingolani, and A. W. Minafra, Phys. Rev. B 5, 1629 (1972).
[40]H. H. Li, J. Phys. Chem. Ref. Data 5, 329 (1976).
[41]J. S. Reid, T. Smith, and W. J. L. Buyers, Phys. Rev. B 1, 1833 (1970).